Investigation of the Roman period pottery production technology from the Seyitömer Mound (Kütahya/Turkey)

V. Uz[1], S. Deniz[1], A. İssi[1] & A. N. Bilgen[2]
[1]Department of Materials Science and Engineering,
Dumlupınar University, Turkey
[2]Department of Archaeology, Dumlupınar University, Turkey

Abstract

The pottery sherds of the Roman period which is the subject of the paper were found at the rescue excavation held in 1989 on site of Seyitömer Mound (Kütahya/Turkey). This study represents archaeometrical analyses of 30 pottery sherds found in the Seyitömer Mound. The important clues for the detection of production and distribution areas of the Roman period sherds were attained in the archaeometrical studies carried out in recent years. A wide variety of characterization techniques were performed. Wavelength dispersive X-ray fluorescence (WDXRF) was performed for chemical analysis, X-ray diffraction (XRD) was performed for mineralogical and phase analysis of the pottery sherds. Scanning electron microscopy (SEM) and microanalysis technique (EDX) were performed for microstructural and microchemical analysis. Thermogravimetric–differential thermal analysis (TG–DTA) was employed for the estimation of firing temperature. Raw materials used for the production, firing temperatures and conditions for the pottery sherds were discussed in the study. From the results obtained, ceramic bodies have been produced from clay deposits rich in iron, containing illitic type minerals and carbonated minerals such as calcite and dolomite. Three groups were concluded as starting raw materials which are rich in calcite, magnesium and siliceous minerals. Firing temperatures of the potsherds change from 600°C to 1100°C.
Keywords: Seyitömer Mound, Roman period, ceramic artifact, characterization, archaeometry.

1   Introduction

Physical and chemical identification of archaeological objects may give a lot of information about ancient civilizations. One of these objects is ceramic. Ceramics used in ancient times could survive till today because of their durability obtained by firing above 400°C. That is why in archaeological excavations, the most recovered materials are ceramics. Investigation of a piece of ceramic could help to reach the information of raw materials, production processes, date and place of production. There are many characterization techniques in a wide variety of enlightening the production technology (Papachristodoulou *et al.* [1], Barone *et al.* [2]).

   The Seyitömer Mound is located 25 km northwest of the centre of Kütahya (Turkey). The Mound is 150x140 m in size and have height of 23.5 m. In order to receive 12 million tonnes of coal reserve under the mound, archaeological excavations is being held in the archaeological site. The archaeological excavations were started under the leadership of Prof. Dr. A. Nejat Bilgen from Department of Archaeology of Dumlupınar University in 2006 after the excavations started in 1989 for a couple of years. It has been enlightened that the Seyitömer Mound has been inhibited by civilizations in the Bronze Age, Achaemenid, Hellenistic and Roman periods (Bilgen [3]). 30 pottery sherds unearthed in the Seyitömer Mound belonging to the Roman period have been investigated. Chemical analysis of samples was performed by wavelength dispersive X-ray fluorescence (WDXRF) and mineralogical/phase composition analysis was performed by X-ray diffraction (XRD) (Vinagre *et al.* [4], Demirel *et al.* [5], Kennett *et al.* [6]) to perform archaeometrical characterization of the artifacts. Scanning electron microscopy (SEM) and energy dispersive spectroscopy (EDS) used for identification of microstructural and microchemical properties of the samples. Thermogravimetric–differential thermal analysis (TG–DTA) was performed to observe the thermal behaviors of the samples to predict the maximum firing temperatures.

Figure 1:   A photograph and a map showing the location of the Seyitömer Mound.

2   Materials and methods

The representative photos of the Roman period samples coded as R17, R18, R19 and R25 were given in Figure 2.
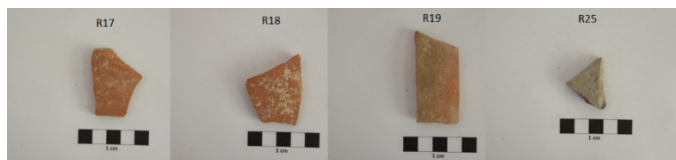
Figure 2:   Photos of R17, R18, R19 and R25 coded samples.

Determined parts of the samples were cut by diamond cutting discs and 0.8–1.5 g of samples were obtained. Samples were stored in deionized water to remove impurities for 2 days. Cleaned samples were dried at room temperature. Powder of the samples was prepared in agate mortars to perform the analysis. A Rigaku Miniflex powder diffractometer with Cu Kα radiation (λ=1.5418 Å) was used for the mineralogical analysis. XRD patterns were obtained by scanning 5° to 55° in 2θ, with a goniometer speed of 2°/min, operating at 40 kV and 30 mA. The interpretation of mineralogical content of the data was conducted with JADE 7 software by searching and matching the powder diffraction files. A Rigaku ZSX primus wavelength dispersive X-ray fluorescence (WDXRF) instrument was used for chemical analysis of the elements. The measurements were carried out on glass tablets prepared by fluxing powdered samples with $Li_2B_4O_7$ in 1:10 weigh ratio. The calculation of the semi-quantitative results was conducted with ZSX software. The results were given as oxides. The microstructural and microchemical aspects of the representative potsherds were investigated using FEI Nova Nano 650 SEM instrument which also includes an EDS detector. Setaram Labsys Evo instrument was used for TG–DTA analysis. A heating rate of 10°C/min was performed in oxidative atmosphere from room temperature to 1200°C.

3   Results and discussions

3.1 Chemical analysis result and discussion

Instead of giving all the results of the study, chemical analysis results belonging to R17, R18, R19 and R25 which are calcium poor and rich and representing chemical analysis of ceramic groups were given in Table 1.

As seen from the results, maximum percentage of CaO belongs to R25 coded sample, minimum percentage belongs to R17 coded sample. Considering total of alkaline and alkaline-earth oxides, R25 have the maximum quantity.

3.2 Mineralogical/phase analysis results and conclusions

XRD results belong to R17, R18, R19 and R25 coded samples given in Table 2. Determined phases are: Quartz (SiO_2), Plagioclase, Illite ((K,H_3O)$Al_2Si_3AlO_{10}(OH)_2$), Microcline ($KAlSi_3O_8$), Calcite ($CaCO_3$), Gehlenite ($Ca_2Al_2SiO_7$), Kaliophilite ($KAlSiO_4$), Augite ($Ca(Mg,Fe)SiO2O6$), Wollastonite ($CaSiO_3$), Akermanite ($Ca_2MgSi_2O_7$), Hematite (α-Fe_2O_3), Maghemite (γ-Fe_20_3), Augite ($Ca(Mg,Fe)SiO_2O_6$). XRD analysis results of R17, R18, R19, R25 coded samples and raw materials of clays are given in Table 2.

Table 1: Chemical analysis results of R17, R18, R19 and R25. The term of "n.d." indicates not detected or under the limits of detection by WDXRF technique performed.

Oxide	Calcium Poor		Calcium Rich	
	R17	R18	R19	R25
Na_2O	0.858	3.1708	2.127	2.847
MgO	0.9629	0.871	4.1693	5.1154
Al_2O_3	18.0834	17.6805	15.02	18.2039
SiO_2	68.2511	66.1349	58.2277	52.6488
P_2O_5	0.0754	0.0651	0.1493	0.2683
SO_3	0.0173	0.0514	0.0867	0.13
Cl	n.d.	0.2851	0.1571	0.1895
K_2O	2.0751	2.0835	2.3857	3.0074
CaO	0.5668	0.5293	6.4215	9.3013
TiO_2	0.9155	0.9445	0.7917	0.8282
Cr_2O_3	0.0487	0.0564	0.3285	0.0711
MnO	0.137	0.1609	0.1421	0.1595
Fe_2O_3	7.8539	7.8184	9.5029	7.0505
NiO	0.0242	0.024	0.1302	0.0425
ZnO	0.0169	0.0146	0.0153	0.0392
SrO	0.0167	0.0152	0.0239	0.028
ZrO_2	0.0381	0.0376	0.019	0.0223
CuO	0.0153	0.0152	n.d.	n.d.
Rb_2O	0.0436	0.0417	n.d.	0.0355
BaO	n.d.	n.d.	0.3023	n.d.
ReO_2	n.d.	n.d.	n.d.	n.d.
HgO	n.d.	n.d.	n.d.	n.d.
As_2O_3	n.d.	n.d.	n.d.	0.0117
TeO_2	n.d.	n.d.	n.d.	n.d.
V_2O_5	n.d.	n.d.	n.d.	n.d.
Co_2O_3	n.d.	n.d.	n.d.	n.d.
PdO	n.d.	n.d.	n.d.	n.d.

Table 2:   XRD analysis results of R17, R18, R19 and R25 coded samples and raw materials of clays.

| Sample Code	Minerals/Phases
R17	Quartz, Microcline, Kaliophilite, Hematite, Maghemite.
R18	Quartz, Microcline, Kaliophilite, Hematite, Maghemite.
R19	Quartz, Plajiyoklas, Illite, Calcite, Wollastonite, Akermanite, Hematite, Maghemite.
R25	Quartz, Plagioclase, Microcline, Illite, Kaliophilite, Augite, Gehlenite, Maghemite.
SNLKKY	Quartz, Plagioclase, Illite/Muscovite, Montmorillonite, Kaolinite, Calcite, Dolomite.
AYVALIB	Quartz, Plagioclase, Illite/Muscovite, Talc, Kaolinite, Kaliophilite, Calcite, Dolomite.
CKOY2B	Quartz, Plagioclase, Illite/Muscovite, Kaolinite/Montmorillonite, Calcite.
IK3A	Quartz, Plagioclase, Illite/Muscovite, Talc, Montmorillonite, Kaolinite, Calcite.
SO1K	Quartz, Plagioclase, Illite/Muscovite, Montmorillonite, Kaolinite, Calcite, Dolomite.
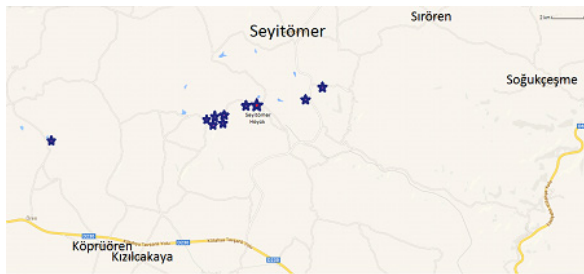
Figure 3:   Shows the raw materials (clays) collected around the Seyitömer Mound.

XRD results of the raw materials (clays) collected around the Seyitömer Mound are also given in Table 2. They were coded as SNLKKY, AYVALIB, CKOY2B, IK3A and SO1K.

Quartz is a mineral with high heat of melting. For this reason, quartz mineral exists in all samples. Quartz and feldspars can persist up to 1000°C (İssi *et al.* [7]). Illite/muscovite or mica structure breaks down in the range of 900–1000°C (Grimshaw [8]). Calcite minerals are decomposed at 850°C. R25 coded sample have no calcite mineral. Therefore, sample might be sintered around 850°C. R19 coded sample includes calcite mineral. It may be fired at lower temperature than decomposition of calcite.

Pyroxenes like diopside and augite may be generated from dolomite and silica reactions at 800–900°C. Gehlenite may be formed at 850°C with the reaction of

CaO and illite structure (Cultrone *et al.* [9]). Gehlenite begins to form at 800°C and disappear at 900°C (Veniale [10]). Wollastonite may be formed at 800°C with the reaction of CaO and quartz structure (Cultrone *et al.* [9]). Sintering temperature is pretty much the same with gehlenite. R19 coded sample which contains wollastonite indicates a firing temperature probably at 800°C. From the decomposition of illite, an intermediate phase originates between spinel ($MgO.Al_2O_3$) and hercynite ($FeO.Al_2O_3$) (Jordan *et al.* [11]). Considering R17 and R18 coded samples are clay based fired bodies, sintering temperature could not exceed 1000°C due to the absence of spinel or mullit phases for samples possible to be generated below 1100°C. Hematite phase in XRD pattern are the signs of oxidative firing (Damjanovic *et al.* [12]). However, existence of maghemite phase on XRD pattern shows reductive atmosphere on firing (Legodi and de Waala [13]).

3.3 SEM analysis results and discussion

SEM images of Ca rich and poor samples are given in Figure 4.

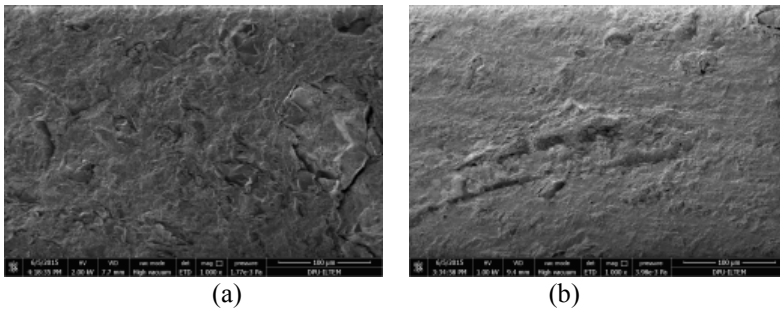(a)   (b)

Figure 4:   SEM images of Ca rich R25 coded sample (a) and Ca poor R18 coded sample (b).

Interactions between clay matrix and grains, shape changes of grains, increase of the aggregation rate within the clay matrix with the formation of secondary porosity and formation of intergranular bridges may be occurred with increasing temperature in clay based ceramics. These changes become more evident in calcareous clays than the siliceous materials including clays (Riccardi *et al.* [14]). Since some of the samples contain high amounts of calcium, SEM images exhibited predominantly arrangements of calcium rich new mineral formations in the microstructure of the samples (Figure 4(a)). Quartz is one of the primary components of clay based ceramics with high melting temperature. It is considered that quartz is relatively insoluble below 1250°C, dissolution of quartz forms silica-rich amorphous solution rims around quartz grains (Iqbal and Lee [15]). Quartz grain dissolution into vitrified clay matrix of the sample may easily be distinguished by the atomic contrast difference in BSE images. Feldspar is believed to melt around 1100°C in the contact zone between feldspar crystals and clay relicts and potash matrix require high temperature around 1200°C.

3.4 Thermogravimetric–differential thermal analysis TG–DTA results and discussion

TG–DTA is one of the convenient methods preferred in characterization of ancient ceramics. This technique allows the examination of changes occurred due to the decomposition, transformation and formation reactions during a controlled heating process (Drebushchak *et al.* [16]). Samples were heated from room temperature to 1200°C with a heating rate of 10°C/min in order to expose the enthalpy changes (plotted by DTA curves with endothermic and exothermic effects) and weight loss/gain (plotted by TG curves).

The endothermic effect from room temperature to 200°C is due to the release of hygroscopic water (Maritan *et al.* [17]). At higher temperatures of 200–300°C the endothermic effect depicts the removal of the chemically bound water, but it may not met in the present study (Paama *et al.* [18]). Depending on the area of the peaks observed in the range of 200–650°C, the exothermic effect identified within these temperatures was attributed to the combustion of organic materials, not completely burnt during firing in reducing condition and transformed into carbonaceous particles which are thought to be deliberately added into the ceramic paste to increase its plasticity or were contained in the clay utilized in the manufacture (Palanivel and Rajesh Kumar [19]). The endothermic effects observed at 700–875°C indicated the decarbonation reactions of mainly calcite and dolomite (Meyvel *et al.* [20]).

TG–DTA results of selected samples are given in Figures 5 and 6.
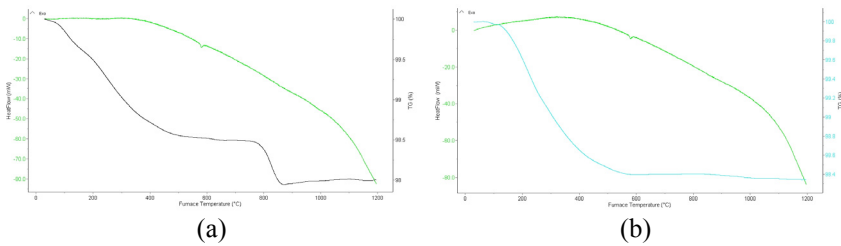

Figure 5:   TG–DTA curve of the sample of R17 (a) and R18 (b).
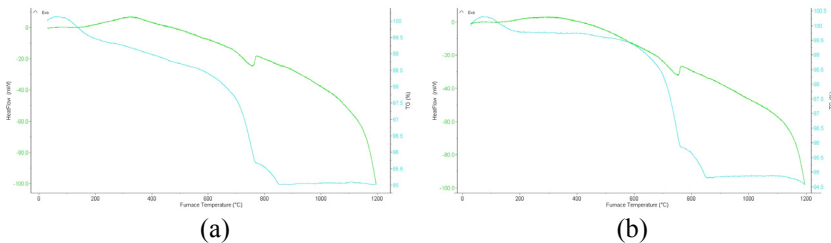

Figure 6:   TG–DTA curve of the sample of R19 (a) and R25 (b).

R17 coded sample has around 2% mass loss. Mass change is methodical up to 450°C. Considering TG analysis with XRD results weight originates from the reactions of unbound or adsorbed water or burning of organic substance. Endothermic reaction in 575°C is because of crystal water decomposition on R17 coded sample. As seen from the Figure 5 mass loss peak is around 1.6% in R18 coded sample. According to TG analysis mass change is methodical up to 420°C. Endothermic reaction in 575°C is because of crystal water decomposition in R18 coded sample. As seen from the Figure 6 mass loss peak is around 5% in R19 coded sample. Mass change is methodical up to 580°C. Endothermic reaction at 750°C may because of calcite decomposition. Mass loss peak is around 5.5% in R25 coded sample. Mass change is methodical to 500°C. Endothermic reaction at 750°C in R25 coded sample may be cause of calcite decomposition again.

4   Conclusions

From WDXRF, XRD, SEM and TG-DTA analysis results obtained, the Roman period ceramics unearthed in the Seyitömer Mound have been produced from clay deposits containing illitic type minerals with rich in iron and calcium rich and poor accessory minerals. To compare with regional geological formations and raw material sources, it may be suggested that local raw material source is enough to produce such kind of ceramic wares during the Roman period. According to phases/minerals in Roman period samples firing temperatures are between 600°C and 1100°C.

Acknowledgement

References

[1]   Papachristodoulou C., Oikonomou A., Ioaniddes K. & Gravani K., A Study of Ancient Pottery by Means of X-Ray Fluorescence Spectroscopy, Multivariate Statistics and Mineralogical Analysis. Analytica Chimica Acta, 573, pp. 347-353, 2006.
[2]   Barone G., Crupi V., Galli S., Majolino D., Migliardo P. & Venuti V., Spectroscopic İnvestigation of Greek Ceramic Artefacts. Journal of Molecular Structure, 651, pp. 449-458, 2003.
[3]   Bilgen, A. N. Seyitömer Höyük Kazısı Ön Raporu. P.1 2011, Kütahya (in Turkish).
[4]   Vinagre U. M., Latini R. M., Bellido A. V. B., Buarque A. & Borges A. M., Ancient Ceramics Analysis by Neutron Activation in Association with Multivare Methods. Brazilian Journal of Physics, 35, pp. 779-781, 2005.

[5] Demirel M., Sevin F. B., Say R. & Yazan Y., Propranolol HCl Imprinted Polymeric Microspheres: Development, Characterization and Dissolution. FABAD J. Pharm. Sci., 32, pp. 147-157, Ankara, 2007.

[6] Kennett D. J., Sakai S., Neff H., Gossett R. & Larson D. O., Compositional Characterisation of Prehistoric Ceramics: A New Approach. Journal of Archaeological Science, 29, pp. 443-455, 2002.

[7] İssi A., Kara A. & Alp A. O., An Investigation of Hellenistic Period Pottery Production Technology from Harabezikan/Turkey. Ceramics International, 37, pp. 2575-2582, Eskişehir, 2011.

[8] Grimshaw R. W., The Chemistry and Physics of Clays. Techbooks, p. 727, India, 1971.

[9] Cultrone G., Navarro C. R., Sebastian E., Cazalla O. & Torre M. J., Carbonate and Silicate Phase Reactions during Ceramic Firing. Eur. J. Mineral, 13, pp. 621-634, Stuttgart (Germany), 2001.

[10] Veniale F., Modern techniques of analysis applied to ancient ceramics. In: Advanced workshop on analytical methodologies for the investigation of damaged Stones. Pavia, (Italy), 1990.

[11] Jordan M. M., Boix A., Sanfeliu T., de la Fuente C., Firing transformations of cretaceous clays used in the manufacturing of ceramic tiles. Appl. Clay Sci., 14, pp. 225-234, 1999.

[12] Damjanovic L., Antunovic I. H., Mioc U. B, Bikic V., Milanovic D. & Evans I. R., Archaeometric study of medieval pottery excavated at Stari (Old) Ras Serbia. J. Archaeol. Sci., 38, pp. 818-828, 2011.

[13] Legodi, M. A. & de Waala M. A., The preparation of magnetite, goethite, hematite and maghemite of pigment quality from mill scale iron waste. Department of Chemistry, University of Pretoria, v.74, i.1, pp. 161-168, Pretoria (South Africa), 2007.

[14] Riccardi M. P., Messiga B. & Duminuco P., An approach to the dynamics of clay firing. Appl. Clay Sci., 15, pp. 393-409, 1999.

[15] Iqbal Y. & Lee W. E., Microstructural evolution in triaxial porcelain. J. Am. Ceram. Soc., 83, pp. 3121-3127, 2000.

[16] Drebushchak V. A., Mylnikova L. N., Drebushchak T. N. & Boldyrev V. V., The investigations of ancient pottery. J. Therm. Anal. Calorim., 82, pp. 617-626, 2005.

[17] Maritan L., Nodari L., Mazzoli C., Milano A. & Russo U., Influence of firing conditions on ceramic products: experimental study on clay rich in organic matter. Appl. Clay Sci., pp. 311-315, 2006.

[18] Paama L., Pitkanen I. & Peramaki P., Analysis of archaeological samples and local clays using ICP-AES, TGDTG and FTIR techniques. Talanta, 51, pp. 349-357, 2000.

[19] Palanivel R. & Rajesh Kumar U., Thermal and spectroscopic analysis of ancient potteries. Rom. J. Phys., 56, pp. 195-208, 2011.

[20] Meyvel S., Sathya P. & Velraj G., Thermal characterization of archaeological potsherds recently excavated in Nedunkur, Tamilnadu, India. Cerâmica, 58, pp. 338-341, 2012.